



Interactions between tectonics erosion and sedimentation during the recent evolution of the Alpine orogen : analogue modeling insights

Cécile Bonnet, Jacques Malavieille, J. Mosar

► To cite this version:

Cécile Bonnet, Jacques Malavieille, J. Mosar. Interactions between tectonics erosion and sedimentation during the recent evolution of the Alpine orogen : analogue modeling insights. *Tectonics*, 2007, 26 (6), pp.TC6016. <10.1029/2006TC002048>. <hal-00404424>

HAL Id: hal-00404424

<https://hal.science/hal-00404424v1>

Submitted on 22 Mar 2021

HAL is a multi-disciplinary open access archive for the deposit and dissemination of scientific research documents, whether they are published or not. The documents may come from teaching and research institutions in France or abroad, or from public or private research centers.

L'archive ouverte pluridisciplinaire **HAL**, est destinée au dépôt et à la diffusion de documents scientifiques de niveau recherche, publiés ou non, émanant des établissements d'enseignement et de recherche français ou étrangers, des laboratoires publics ou privés.



HAL Authorization

Interactions between tectonics, erosion, and sedimentation during the recent evolution of the Alpine orogen: Analogue modeling insights

Cécile Bonnet,¹ Jacques Malavieille,² and Jon Mosar³

Received 8 September 2006; revised 24 July 2007; accepted 4 October 2007; published 29 December 2007.

[1] On the basis of a section across the northwestern Alpine wedge and foreland basin, analogue modeling is used to investigate the impact of surface processes on the orogenic evolution. The basis model takes into account both structural and lithological heritages of the wedge. During shortening, erosion and sedimentation are performed to maintain a critical wedge. Frontal accretion leads to the development of a foreland thrust belt; underplating leads to the formation of an antiformal nappe stack in the internal zones. Important volumes of analogue materials are eroded out of the geological record, which in the case of the Alps suggests that the original lengths and volumes may be underestimated. The foreland basin evolves differently depending on the amounts of erosion/sedimentation. Its evolution and internal structuring is governed by the wedge mechanics, thought to be the main controlling mechanism in the development of the Molasse basin in a feedback interaction with surface processes. **Citation:** Bonnet, C., J. Malavieille, and J. Mosar (2007), Interactions between tectonics, erosion, and sedimentation during the recent evolution of the Alpine orogen: Analogue modeling insights, *Tectonics*, 26, TC6016, doi:10.1029/2006TC002048.

1. Introduction and Scope of the Study

[2] In the Alps feedback mechanisms linking surface processes, tectonic processes and structural heritage can be investigated at first hand. The Molasse foreland basin develops in the northern part of the orogen in response to the development of the mountain belt and receives the products of the erosion of the orogenic belt. The basin structure not only reflects the Tertiary history of the Alps, but also responds to the mechanics of the orogenic wedge. Indeed, the size of the basin, which is considered here as part of the wedge, influences the wedge mechanics such as for instance the sequence of thrusting. The exhumation of the External Crystalline basement Massifs, south of the

Molasse Basin is largely driven by the subduction mechanism of the European plate under the Adriatic promontory. However, it appears that erosion of the overlying Penninic orogenic lid controls the localization, the velocity and magnitude of the exhumation. To the north of the Molasse Basin, the Jura foreland fold-and-thrust belt started to form during the Miocene, because of a major “jump” of the Alpine thrust front by about 100 km toward the north under the Molasse foreland basin. This foreland directed propagation of the frontal thrust is due to a combined effect of the structural and lithological settings and the shape of the Molasse Basin; hence the nature and amount of sedimentation. Among other causes, the presence of a large thickness of Molasse deposits in the Alpine foreland allowed the activation as décollement level of the Triassic evaporite layers accumulated at the base of the European cover. The Alpine development of the orogenic wedge is further strongly influenced by a structural heritage of Mesozoic sedimentary half-graben type basins developed along major normal fault systems. In order to understand the complex interactions between erosion, sedimentation, structural heritage and tectonics and to investigate the importance of sedimentation/erosion, we performed a series of analogue models.

[3] Geodynamics of orogenic wedges has been for a number of years a major subject of research [Beaumont *et al.*, 1996; Dahlen *et al.*, 1984; Davis *et al.*, 1983; Konstantinovskaia and Malavieille, 2005; Mattauer, 1986; Molnar and Lyon-Caen, 1988; Willett, 1992]. The case of the Alpine mountain belt is a very well established and documented example of internal dynamics [Escher and Beaumont, 1997]. Studies have focused on the mechanics of the Alpine orogenic wedge [Pfiffner *et al.*, 2000] and on the complex interactions between tectonics and surface processes and their consequences on both the dynamics of the orogenic wedge and the evolution of topography [Beaumont *et al.*, 2000; Cederbom *et al.*, 2004; Kooi and Beaumont, 1996; Kühni and Pfiffner, 2001; Persson and Sokoutis, 2002; Pfiffner *et al.*, 2002; Schlunegger, 1999; Schlunegger and Hinderer, 2001, 2003; Schlunegger *et al.*, 1997, 1998; Storti and MacClay, 1995]. Depending on their rates and localization in space and time, erosion and sedimentation modify the morphology and the internal structure of the wedge. Geological and geophysical studies do provide a global view of the Alpine orogenic wedge at a lithospheric scale, but this image is a “snapshot” in time. Numerical and analogue modeling offers the possibility for a complete and direct observation of scaled models simulating geologic features developed over geologic timescales

¹Department of Earth Science, University of California, Santa Barbara, California, USA.

²Geosciences Montpellier, Université Montpellier II, Montpellier, France.

³Department of Geosciences—Earth Sciences, University of Fribourg, Fribourg, Switzerland.

and often in subsurface. Thus modeling appears to be appropriate to study and quantify dynamically the impact of surface processes on the evolution of the wedge. It allows systematic tests on models varying mechanical and geometrical parameters that are difficult to analyze.

[4] To study the evolution of the Alpine mountain belt and investigate the influence of surface processes on tectonics, a series of scaled analogue experiments have been performed. This type of analogue models obeys the dynamics of a critically tapered wedge and the structures produced inside the wedge are determined by the wedge mechanics. The criticality of the taper may be influenced by outside processes such as erosion and sedimentation. Our experimental approach is new since our models take into account the regional structure of the wedge. In our experiments we analyze the role and interactions of the initial inherited structures, the rheologies, the erosion and the sedimentation on the Alpine orogenic evolution, including the Molasse foreland basin.

[5] First we will describe the initial structural setup, based on a restored section across the Western Alps from *Burkhard and Sommaruga* [1998]. Then the geometries of the developed structures and their evolution in space and time will be linked with the involved tectonic processes and compared with the Alpine development. A semiquantitative analysis of the experimental sediment budget and its evolution through time are linked to the dynamical framework of the growing wedge. Finally we discuss the interactions between surface processes, structural and lithological heritages and tectonic processes, as well as their feedback on the dynamics of the Alpine wedge.

[6] The goal of our study was to determine the importance of inherited structures (in the basement and cover) in the development of an orogenic wedge and investigate the influence of surface processes such as erosion and sedimentation on the evolution and structuring of the foreland basin and the hinterland.

2. Orogen-Foreland Basin System: Alps and Modeling Setup

[7] A detailed review of the evolution of the Alpine orogeny is beyond the scope of this paper (for detail, see cited references). Rather, we will point out some points noteworthy for the understanding and discussion on the evolution of the orogenic wedge and the comparisons with our analogue models.

2.1. Geological Framework of the NW Swiss Alps

[8] On the basis, mainly, of the tectono-metamorphic activity [*Dal Piaz et al.*, 1972; *Escher and Beaumont*, 1997; *Escher et al.*, 1997; *Hunziker et al.*, 1989, 1992; *Mosar*, 1999; *Mosar et al.*, 1996; *Schmid et al.*, 1996; *Stampfli et al.*, 1998a; *Steck and Hunziker*, 1994; *Trümpy*, 1973, 1980] Alpine evolution can be subdivided into three main orogenic phases: the Eoalpine events, Cretaceous to Early Paleocene in age (140–60 Ma), the Mesoalpine events, of Late Paleocene to Early Oligocene age (60–30 Ma) and the Neoalpine orogenic events, of Late Oligocene and

younger age (30–0 Ma). The last two phases and mainly the Eoalpine phase correspond to the period during which the Alpine foreland basin develops from an underfilled Flysch Basin to an overfilled Molasse Basin [*Homewood and Lateltin*, 1988; *Sinclair*, 1997]. It is during these younger events that the main mountain building processes operate. It is these processes and their interaction with the foreland basin evolution and the hinterland orogenic structuring that we intended to investigate in our analogue models.

[9] During the Eoalpine event the subduction of the Alpine Tethys and Valais Oceans lead to the progressive closure of the Alpine Tethys. An aerial orogeny developed owing to the continental subduction of the European plate under the Apulia/Adria plate [*Escher et al.*, 1997; *Schmid et al.*, 1996; *Stampfli et al.*, 1998a, 1998b]. In the upper plate, the stacking of the Austroalpine nappes creates the initial orogenic lid.

[10] During the Mesoalpine orogenic events, the Briançonnais and subsequently the internal part of the European continental crust will be incorporated into the accretionary prism and will be part of the upper plate orogenic lid [*Escher et al.*, 1993; *Schmid et al.*, 2004]. This resulted in the formation and stacking of basement nappes. The tectonic inversion of the inherited normal faults forming the Mesozoic basin [*Funk and Loup*, 1992; *Trümpy*, 1960] played a major role during this event. At the end of the Mesoalpine period, the internal European crustal units were thrust by tectonic underplating below the external Briançonnais units thus moving into the upper plate. Simultaneously, the first Helvetic nappes began to take shape.

[11] During the Neoalpine orogenic event, starting around 30 Ma ago, continued frontal accretion and imbrication of thrust units is coincident with the development of S and SE-vergent backthrusting and backfolding in the overriding orogenic lid [*Escher and Beaumont*, 1997]. The northwest and southeast movements produced a generalized exhumation and erosion with deposition of Molasse sediments in peripheral foredeep basins. During the uplift of the External Crystalline basement Massifs, the Prealpes klippen were disconnected from their Penninic homeland farther south.

2.2. Framework for the Experimental Setup

[12] The framework of the experimental study is based on a transversal section across the western Alps (Figures 1a and 1b) that extends from Besançon in the NW to Torino in the SE. This transect (Figure 1b) is based on seismic-reflection profiles [*Sommaruga*, 1997], surface-geology and thrust-system considerations [*Burkhard and Sommaruga*, 1998]. The restored profile (Figure 1c) along this section highlights the inherited structural features of the European basement. The structural and lithological heritages play a major role in the kinematic and geometric development of the belt. It was therefore important to take into account the prestructuring of the basement units and the sedimentary cover, in the experimental set up. Further, our modeling intends to investigate the inversion of the European platform and the development of the external parts of the Alpine

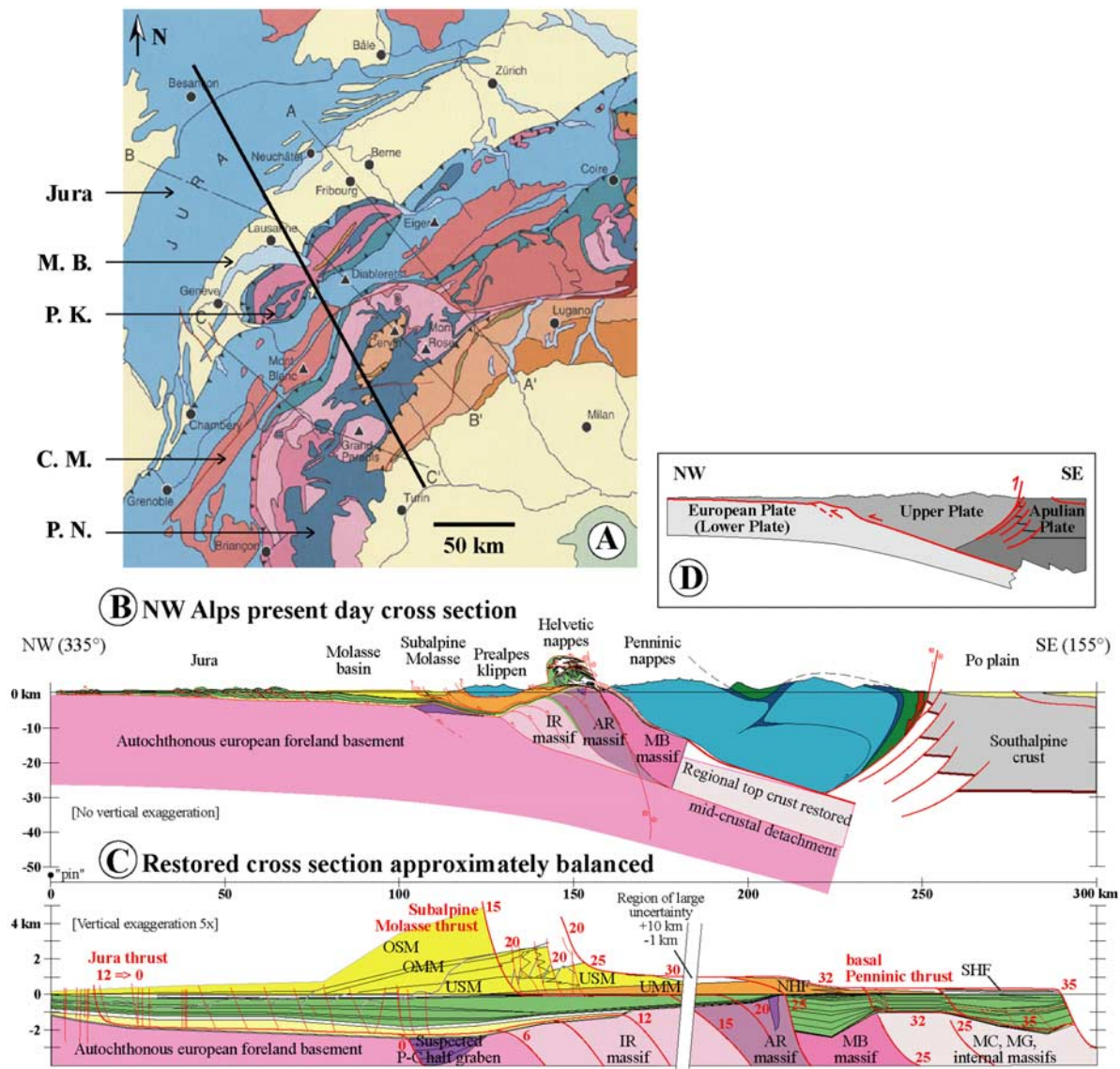


Figure 1. Location map and transversal section across the NW Alps used as experimental basic model. (a) Localization of the section and succession of structural units on a tectonic map of the Alps [Schmid *et al.*, 2004]. (b) NW Alps present-day cross section [Burkhard and Sommaruga, 1998] with the converging European plate composed of successive basement units (pink) and their Mesozoic cover (blue, orange, and yellow) and the Apulian upper plate constituted at its front mainly by the Penninic nappes (light blue) from which the Prealpes klippen are detached. (c) Restored cross section approximately balanced [Burkhard and Sommaruga, 1998] showing the prestructured basement units and sedimentary basins of the Helvetic domain, the weak layer of Triassic evaporites at the base of the cover, the estimated volumes of overlying Molasse deposits, and the thrust at the base of the overriding Penninic lid. (d) Simplified sketch of the upper versus lower plate configuration of the Alpine orogen.

orogen including the Jura, the Molasse Basin and the External Basements and their Helvetic cover units. The overriding Penninic and Austroalpine units are considered as one structural unit forming the orogenic lid (proto-wedge in Figure 2).

[13] The main structural features are as follows. (1) A crystalline basement is dipping gently from the foreland toward the orogen. (2) Localized grabens are filled with

Carboniferous and Permian clastics, considered as the last expression of the Variscan orogeny. (3) A passive margin series deposited at the southern margin of the European plate above a major “post-Variscan” erosional unconformity is constituted by Middle Triassic to Upper Cretaceous shallow-marine carbonates. It includes the future Jura, Molasse, “Autochthonous” and Helvetic domains and has a total thickness varying from 1 to 2.5 km [Loup, 1992;

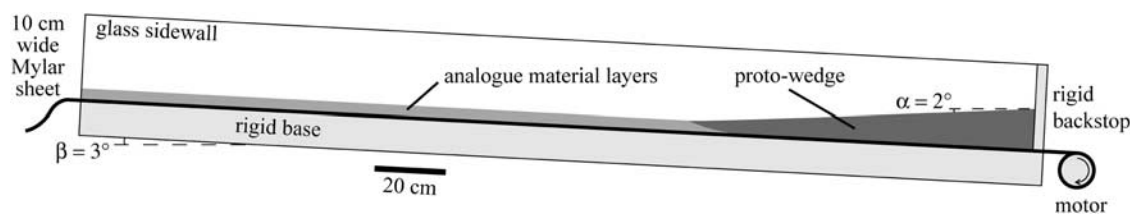


Figure 2. Experimental sandbox device and basic setup simulating the development of a foreland basin in front of a growing orogen, based on a model Coulomb wedge (on the scheme, surface (α) dips 2° to the left, and base (β) 3° to the right, corresponding respectively to 2° to the north and 3° to the south in an Alpine setting). Prestructured analogue materials are pulled on a Mylar sheet against a rigid backstop leading to the development of a thrust wedge.

Wildi et al., 1991]. (4) Tertiary clastic wedges are deposited above a well-developed foreland unconformity which can be traced from the external Jura southward into the most internal Helvetic domain [Boyer and Elliott, 1982; Herb, 1988; Homewood et al., 1989]. (5) The lateral continuity between Helvetic and Molasse parts of the foreland basin has been obscured by incorporation into the evolving orogenic prism. The tectonic activity progressively advanced from the internal parts toward the northwest including Penninic, Helvetic and Subalpine Molasse thrust systems [Burkhard, 1988; Pfiffner, 1986].

[14] Some important points in the evolution of the wedge are as follows. (1) In the late Eocene (~ 40 Ma), foreland sedimentation started in the most internal (Helvetic) domain in a shallow (<600 m deep) and narrow (<100 km wide) underfilled trough, before being subsequently buried by the overriding Penninic (including Ultrahelvetic) thrust front [Burkhard and Sommaruga, 1998]. (2) In the latest Eocene (~ 40 to 30 Ma), the thrust front and the “pinch-out” (Figure 1) advanced very quickly northwestward and the basin grew to about 100 km width. In the early Oligocene (~ 30 to 22 Ma), both thrust front and “pinch-out” migrated at the same decreased rate, maintaining constant the basin width. During this same period the basin went from underfilled Flysch Basin to overfilled Molasse Basin. (3) Simultaneously the crystalline basement units started develop, strongly influenced by the tectonic inversion of previous normal faults [Escher et al., 1997]. (4) The onset of main Jura deformation is generally proposed to start in the Late Miocene, after the Serravalian [Burkhard, 1990; Laubscher, 1987, 1992; Naef et al., 1985] following a “jump” of the thrust front from within the Molasse Basin to its northern side. During the thrusting of the Jura, the Aar massif culmination has about half its present amplitude [Burkhard and Sommaruga, 1998]. Also, the development of the thin-skinned frontal fold-and-thrust belt of the Jura is strongly linked to the décollement in the Triassic evaporites, and involves a distant push from the Alps, called “Fernschub theory” [Boyer and Elliott, 1982; Burkhard and Sommaruga, 1998; Buxtorf, 1916; Laubscher, 1973]. (5) The geodynamic development of the Alpine foreland has been continuous through time and goes on consequently at the present day [Lacombe and Mouthereau, 2002; Mosar, 1999].

[15] Uncertainties remain as to the detailed geometry of the structures below the Prealpes klippen in Western Swit-

zerland. On the basis of different types of seismic data it is suggested that the basement rises to form a structural high beneath the Western Prealpes Romandes (Switzerland) and the Eastern Chablais Prealpes (Switzerland and France) [Mosar, 1999]. The same data suggest a possible inversion of a Permo-Carboniferous graben beneath the transition from the Molasse to the Prealpes klippen (Subalpine flysch) in the Rhone valley area [Burkhard and Sommaruga, 1998; Gorin et al., 1993; Sommaruga, 1997, 1999].

3. Apparatus, Experimental Procedure, and Results

[16] Analogue modeling investigations using granular materials have shown the similarity between deformation in model wedges and structures observed in fold-and-thrust belts and/or submarine accretionary wedges [e.g., Davis et al., 1983; Malavieille, 1984]. Subsequent studies have been led to systematically investigate the role of main experimental parameters such as for instance basal friction, layer thickness, sediment rheology, brittle-ductile coupling, relative strength of the backstop material, taper geometries and ratio of sediment input to output (nonexhaustive list of publications: [Byrne et al., 1988; Cobbold et al., 2001; Gutscher et al., 1998a; 1998b; Konstantinovskaia and Malavieille, 2005; Lallemand et al., 1994; Liu et al., 1992; Mulugeta, 1988; Persson and Sokoutis, 2002; Smit et al., 2003; Storti and MacClay, 1995]).

3.1. Experimental Setup and Procedure

[17] Our original study investigates the structural evolution of model setup based on a section across the Western Alpine accretionary wedge, under given experimental conditions of erosion/sedimentation, and especially taking into account the inherited regional structure. The structural heritage is both tectonic, with faults of inherited basins that can be reactivated as reverse faults, and stratigraphic, with the succession of contrasted lithologies. The experimental setup of our analogue model is constrained by the restored section proposed by Burkhard and Sommaruga [1998]. We wish to insist that our approach is a first-order study, and that the initial state and boundary conditions of this simulation of the Alpine setting and development remain a simplification of a very complex natural setting.

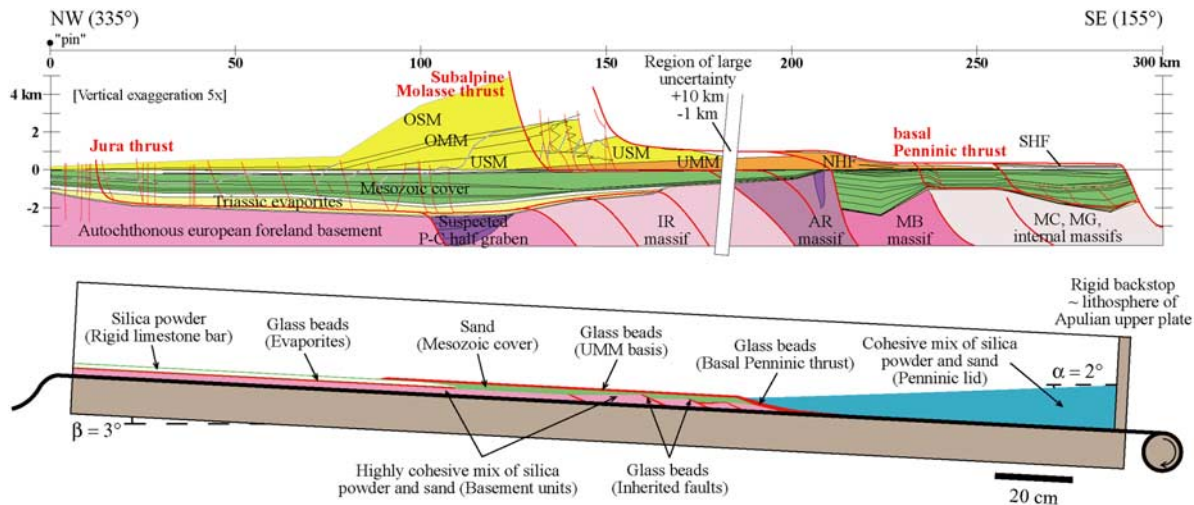


Figure 3. Structural setup based on the restored section across the Western Alps by *Burkhard and Sommaruga* [1998]. On the right side, the upper plate represented by a homogeneous solid lid (blue) will override on a basal thrust (red) the lower plate constituted by a succession of solid basement units (pink) and their more “deformable” cover (green), both prestructured by inherited faults (red). A rigid layer (white) located in the core of the cover mimics a calcareous horizon and is underlain by a weak level (red) simulating evaporites at the base of the Mesozoic cover.

[18] Descriptions and estimates of the postcollisional sediment budget history of the western and central parts of the Alps have been proposed by some authors [*Kuhlemann*, 2000; *Kuhlemann et al.*, 2001, 2002; *Kuhlemann and Kempf*, 2002]. We did not impose given rates of erosion and sedimentation in our experiments based on these studies since it is still debated what is the cause of increased erosion and sedimentation in order to investigate the feedback influence of surface processes on wedge mechanics.

[19] The experiments were performed under normal gravity in a classical sandbox device, close to the set up elaborated by *Malavieille* [1984]. The device (Figure 2) is formed by a flat rigid base bound by two lateral glass walls. A motor pulls on the plate a 10 cm wide Mylar sheet with a rough surface simulating a high basal friction. Analogue materials are deposited on the sheet to fit the succession of units present on the restored cross section of the western Alps. The shortening leads to the development of the analogue thrust wedge against a rigid backstop, with no subduction window at its base. The layers of analogue materials mimic the subducting European plate, while the proto-wedge represents the Penninic orogenic lid that will be deformed against the rigid backstop simulating the strong lithosphere of the Apulian upper plate (Figures 1d and 3). Cohesion and size of material are scaled with a factor of 10^5 (for scaling and characterization of model materials, see also *Gutscher et al.* [1998a], *Gutscher et al.* [1996], *Kukowski et al.* [2002], and *Lallemand et al.* [1994]; for additional references, see *Lohrmann et al.* [2003]). The length of the basal plate (about 2.80 m) offers a maximum convergence of 160 cm that corresponds to 60% of shortening or about 400 km at the natural convergent orogenic wedge scale. One

camera records all stages of the experiment allowing structural interpretations and semiquantitative analysis to be made.

[20] The “critical wedge” theory [*Dahlen*, 1984; *Dahlen et al.*, 1984; *Davis et al.*, 1983] predicts that the geometry of a growing wedge (defined by its surface slope α and its basal slope β) is a function of the material strength and the basal friction. Deformation in accretionary wedges (with negligible cohesion) is consequently scale independent. As orogens are on the verge of gravitational failure [*Davis et al.*, 1983], they adopt a distinct geometry with a low-tapered pro-wedge facing the subduction plate, and a high-tapered retro-side [*Willett et al.*, 1993]. The model Coulomb wedge used in the experiments (Figure 2) presents the geometry of the Alpine proto-wedge proposed in cross sections of the literature [*Lacombe and Mouthereau*, 2002; *Mosar*, 1999]: the surface of the wedge (α) dips 2° to the north and the base (β) dips 3° to the south, which corresponds to the dip of the subducting European plate. The easiest solution to simulate the basal dip was to incline the experimental device which is a major simplification since we do not consider lithospheric flexure. The behavior of the deep ductile part of the crust was not considered here since only its upper part is involved in the deformation. Indeed, as can be seen on most deep seismic reflection profiles crossing the Alps [*Guellec et al.*, 1990; *Mugnier et al.*, 1990; *Pfiffner et al.*, 1990], a midcrustal detachment level is located above the well-layered lower crust [*Burkhard and Sommaruga*, 1998].

[21] The analogue materials have frictional properties satisfying the Coulomb theory [*Dahlen*, 1984; *Dahlen et al.*, 1984; *Davis et al.*, 1983] and they mimic a nonlinear deformation behavior of crustal rocks in the brittle field [*Lohrmann et al.*, 2003]. The three kinds of used materials (sand, silica powder and glass beads) are chosen for their

contrasted behaviors and are employed both mixed and separately to fit the behavior of different tectonic and stratigraphic units. The aeolian sand used in this study is rounded with a grain size of 200 to 315 μm and a density of 1690 kg/m^3 . The internal coefficient of friction is 0.57 and the cohesion $C_0 = 20$ Pa. Décollement levels are created by introducing in the model layers of glass beads with a grain size between 50 and 105 μm . They are a Coulomb material and their density is almost the same as that of dry sand. However, owing to their close to perfect roundness their coefficient of internal friction is about 23% smaller (0.44), with cohesion almost negligible. Resistant layers in the models are made of pure dry silica powder or of a mix with sand. Silica powder has a significantly higher cohesion (150 Pa) than sprinkled sand (20 Pa) and may simulate stronger (resistant) material. The solid units, i.e., the orogenic lid (Penninic) and the basement units (Figure 3), are a very cohesive mix of silica powder and sand in variable proportions. The lid is passively transported and eroded, and its internal structure does not appear to play a major role in the tectonic development of the wedge. Consequently, and in order to keep the model simple, we did not differentiate cover and basement units in the Penninic. In the foreland, different units corresponding to the various Crystalline Massifs were distinguished (Figure 3). There equivalent more “deformable” cover units are composed of sprinkled sand only, and correspond to the Mesozoic cover of the European margin between the Jura platform and Helvetic/Ultrahelvetic margin. In the central part of the cover layer, a level of cohesive pure silica powder (Figure 3) simulates a rigid calcareous horizon (Tithonian limestones of the Jura). Thin (<2 mm) layers of glass beads are used to create weak zones simulating preexisting inherited faults and décollement levels such as the basal detachment in the Triassic. According to reconstruction of the Mesozoic depocenters, the major inherited normal faults are south-dipping, juxtaposing basement units with cover sediments (Figure 3). In our experiment, these décollement levels play as reverse faults, as in the Alpine orogen. Another glass bead layer is placed at the base of the sand, under the pure silica powder level (Figure 3). It mimics the Triassic evaporites that behave as décollement level for the cover during the shortening. The last thick (<8 mm) décollement level of glass beads allows the orogenic lid to override the basement and cover units (Figure 3). It corresponds to the basal Penninic thrust associated with detachment level associated to the Ultrahelvetic series.

[22] In the models, erosion was imposed to maintain a more or less constant slope of the wedge geometry, thus keeping a mechanical equilibrium of the wedge. After each experimental increment, an average surface slope of several degrees (2° – 4°) is used to determine which domains of the wedge will be subjected to erosion. A model test run with similar initial setup, but no erosion, develops a critical wedge with slopes of the same inclination as those observed in the model described herein (surface slopes around 2° – 6°). Erosion was performed using a vacuum cleaner, and is independent of the lithological nature of the units. Only the topography above this average limits, the height

perturbations, will be eroded. This is also supported by the observation that the rate of erosion can be positively correlated with local relief [Hooke, 2003; Summerfield and Hulton, 1994]. In a general way erosion is in the regions where topography is building, but from our models we have not determined if erosion is increasing linearly toward higher topographies, which would then be similar to simple erosion models, where erosion is distributed and possibly even linearly dependant on elevation [Hoth et al., 2004; Konstantinovskaia and Malavieille, 2005]. Sedimentation is done in the foreland in the basin and on the deforming orogenic front (developing piggyback basins) by sprinkling sand to fill the same 2° – 4° average surface as used for erosion. Generally, the undeformed part of the foreland basin has a shallower surface dip as the trailing deformed/imbricated portion.

[23] Though simplified, we were careful to obtain realistic rates of erosion and sedimentation. For instance, at the end of the experiment, the deposited volumes still in the geological record constitute 10% to 20% of the eroded volumes, as proposed in the literature [Kuhlemann, 2000; Kuhlemann et al., 2001, 2002; Kuhlemann and Kempf, 2002]. The scaled volumes of analogue materials involved in the sediment budget history may be then compared to the values proposed for the Alpine sediment budget. The major part of the eroded material exits the system, as it does in nature in the Alpine system, where large rivers helped carry most of the eroded sediments away and out of the Molasse Basin system.

[24] The quantitative data presented on the various graphs may be impinged by small errors related to different sources like the experimental procedure, the mechanical properties of the used materials and the transition between the machine and the graphical representation. Because of the uncertainty related to the estimation of the errors and because they remain small to negligible and may be either added or subtracted, no error bars have been presented on the graphs. The experiments have been performed with incremental displacements of the basal Mylar sheet (stop at each 2 cm), measured on a graduated ruler with a maximal error of 5% (1 mm for each increment, but with a total length of the experimental setup of 280 cm). Despite its mechanical resistance, the long Mylar sheet may be slightly stretched owing to the increasing force of traction necessary to pull the growing wedge. Since there is no evidence of a consistent and/or proportional relationship between the length of the Mylar sheet and the displacement of materials, it seems that stretching of the sheet is negligible. Friction on the lateral glass walls during displacement of the material is diminished thanks to the application of a lubricant before material deposition. A slight diffusion leading to a less precise reading of markers cannot, however, be excluded. Another kind of error results from the graphical analysis. The localization of a particle and the drawing of a line or surface by the same person are not exactly reproducible from one stage to the other. The error estimated on distances is less than 1% and on areas less than 2%. Finally, the error due to the change of scale between the analyses performed on photographs and the studied features on the machine is

estimated to 1.3%. Compared to the approximations at the base of the model setup and to the simple laws used in the experimental procedure, the different errors of measurements are considered negligible.

[25] We performed a series of seventeen experiments, the first 11 of which eventually led to a satisfying basic model presented previously (Figure 3). We varied unit's lengths, angles, rheologies and localization of décollement levels to constrain the geometry and mechanical behavior of the different tectonic units and depositional realms. In the last six experiments, we varied the rates of sedimentation and erosion to better understand the influence of surface processes on the evolution of a mountain belt.

3.2. Experimental Results

[26] In the following, we describe the evolution of one of these last experiments, for which the imposed erosion and sedimentation pattern led to a two-dimensional development best reflecting the geometries observed along the proposed of the studied cross section of the Western Alps (auxiliary material Animation S1¹). Displacement of the subducting plate is described in terms of time increments. The 152 cm of subducting plate convergence in the model correspond to 380 km of natural displacement of the European plate, and are performed between the time increments t_0 and t_{38} (Figure 4).

[27] The rates and localization of erosion and sedimentation vary during the experiment in response to the tectonic development of the model. To simulate the submarine episode of the orogen before continental subduction, the initial stage of the experiment (t_0 to t_5) was achieved with no erosion/sedimentation. Then the orogen becomes aerial (t_6) and this until the end of the experiment. Erosion is performed to preserve the regular initial slope of the wedge, both on the lid and on the recently deposited foreland sediments. Simultaneously in the foreland, the successive layers of sedimentary filling are added to obtain the equilibrium profile.

[28] From the beginning, model shortening leads to thrusting of the lid on top of the basement/cover units. The geometrical response is a continuous and marked internal deformation of the lid due to retrothrusting (t_{10} , Figure 4). The nucleation of retrothrusts takes place at the transition from flat to ramp of the basal thrust of the lid. Backthrusts are active as long as they are located on this mobile transition point. They are subsequently passively displaced on the top of the ramp, becoming inactive (t_{16} , Figure 4). At an advanced stage of the experiment (t_{29} , Figure 4), we may notice that some former retrothrusts are reworked by new ones generated at a transition from flat to ramp inside the basement units.

[29] The displacement of the orogenic front is first accommodated by several small thrust slices in the foreland sediments, very close of the lid front (t_{10} , Figure 4). The deformation is then propagated to the foreland (t_{13} , Figure 4) owing to the activation of the décollement level, simulated

by a glass bead layer at the base of the foreland basin. The displacement of the orogenic front is accommodated by retrothrusting and a small piggyback basin grows in the trailing part of a frontal pop-up structure (t_{16} , Figure 4).

[30] From stage t_{16} on (Figure 4), the inherited structural grain controls the deformation of the subducting plate. The different décollement weaknesses, simulating the inherited normal faults and surrounding basins, are activated as reverse faults in the basement units. These faults propagate across the basal décollement level and appear at the surface as a succession of foreland sediment slices. Then the basement imbricates thrust each other according to a process called underplating (t_{23} , Figure 4). This mechanism allows material of the lower subducting plate to be accreted into the upper plate [Gutscher *et al.*, 1996; Kukowski *et al.*, 2002; Platt, 1986].

[31] At stage t_{29} (Figure 4), following the evolution of the prestructured basement units, the homogeneous, not prestructured part of basement of the subducting plate is spontaneously underplated. The resulting thrust affects both the sedimentary cover and the overlying foreland sediments. It initiates a fold-and-thrust development in the foreland. The combined effect of tectonics and erosion leads to localization of the uplift on basement units and the isolated front of the lid constitutes a nappe (t_{29} , Figure 4). At this stage of evolution, the piggyback basin located on the frontal part of the lid is completely eroded. On the final stage picture (t_{38} , Figure 4), the development of the fold-and-thrust belt in the foreland constitutes the last event of the orogenic evolution. The different units have been largely eroded and more particularly the foreland basin, the Penninic lid and also its frontal isolated nappe. The underplating of the basement units has led to the formation of an antiformal nappe stack.

4. Interpretation of Results

[32] The evolution of the experiment may be described by three major tectonic phases. From t_0 to t_{15} , the lid climbs up onto the top of the basement ramp owing to the subduction of the converging plate. Then, from t_{16} to t_{28} , the wedge grows by underplating of the prestructured basement units. In the following chapters, this phase will be called “underplating of the Crystalline Massifs” in reference to the cross section by Burkhard and Sommaruga [1998]. The final tectonic phase, from t_{29} to t_{38} , is marked by the spontaneous underplating of the unstructured part of the basement. Similarly, in reference to the Alpine setting, this phase will be called “underplating of the Autochthonous European basement.”

4.1. Experimental Results (Tectonic and Structural) Versus Observed Structures

[33] A comparison between the model at a very advanced stage of its evolution (t_{34}) and the basic cross section (Figure 5a) reveals that the first-order tectonic structures that developed present similar geometries. The antiformal geometry of the basement nappe stack is similar to the profile from Burkhard and Sommaruga [1998], who suggest

¹Auxiliary materials are available in the HTML. doi:10.1029/2006TC002048.

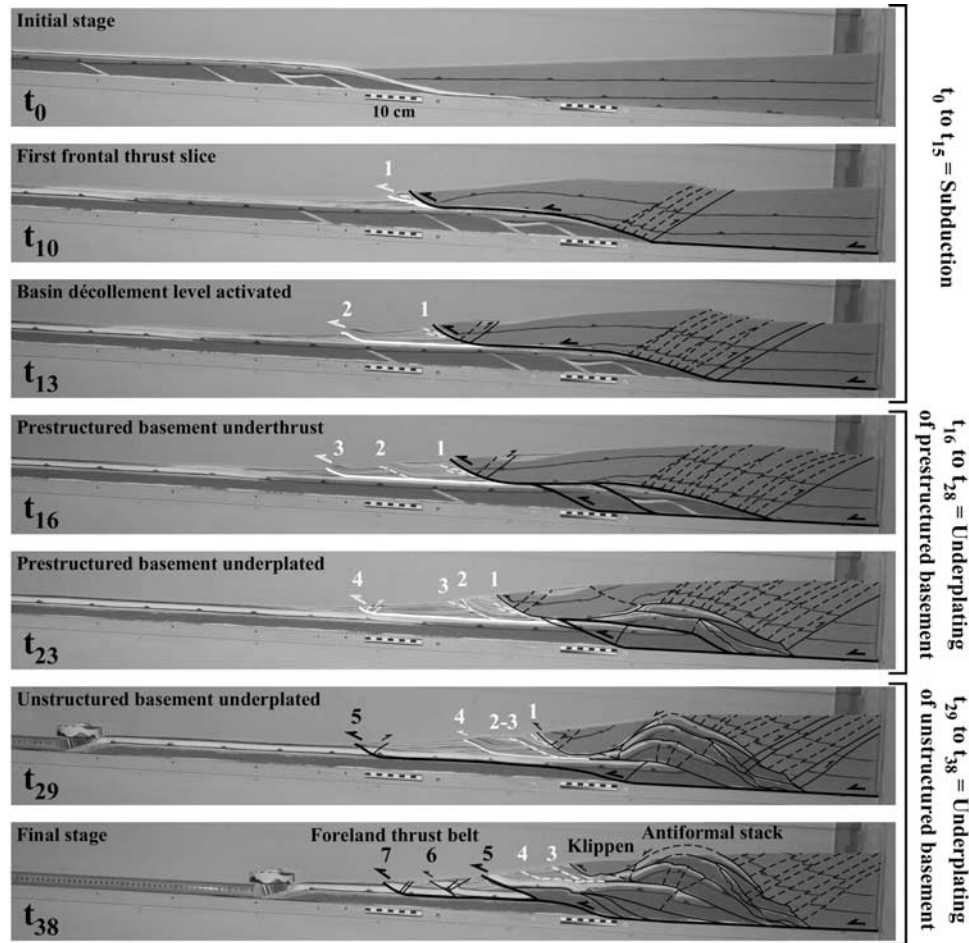


Figure 4. Key stages of the analogue model evolution from time increment t_0 to t_{38} . Structural interpretation is wrapped on the pictures: thrust affecting only the foreland sediments (white); other faults, i.e., affecting the lid, the basement units, and the cover (black); faults accommodating major displacements (thick lines), minor displacement (thin lines), and inactive faults (dashed lines). Here t_0 is initial stage; t_{10} is climb of the lid onto the top of the basement ramp causing an intense internal deformation of the lid due to backthrusting; t_{13} is first slice of recently deposited foreland sediments thanks to the activation of the basal décollement level in the basin; t_{16} is inversion of the inherited basement normal faults and propagation to the surface as a second foreland sediment slice; t_{23} is underplating of the basement imbricates and development of a third foreland sediment slice; t_{29} is spontaneous underplating of the homogeneous part of the basement, initiation of a fold-and-thrust development in the foreland, and detachment of a nappe from the lid due to the uplift of basement units; and t_{38} is final stage picture showing the developed foreland fold-and-thrust belt, the remains of the detached nappe and the antiformal basement nappe stack.

that thrust ramps and stacking with more than 36 km of combined horizontal shortening are responsible for the formation of the External Crystalline Massif culmination. In addition, to accommodate the whole proposed total shortening, they show on the present-day cross section trapped Mesozoic cover between the basement imbricates (Figure 5a, top). Similar features are identifiable also in the experiment: considerable shortening is distributed on the different thrust planes and cover units appear between the basement nappes (Figure 5b). As is the case for the Helvetic cover nappes, such as the Morcles nappe with its crystalline core formed by the Mt Blanc massif (Figure 5a,

top), in the experimental antiformal nappe stack, the cover of the two most internal basement units underwent similarly a large displacement. The transport of this cover nappe even brought its upper part to the surface, where it is eroded (Figure 5b).

[34] The uplift of the basement nappe stack causes a klippen to detach from the main body of the orogenic lid. This tectonic unit, very similar to the Prealpes klippen (Figure 5a) in terms of geometry, location, dimensions and mechanism of emplacement, illustrates well how the mechanisms of nappe emplacement are strongly influenced by erosional processes. A major difference is that the

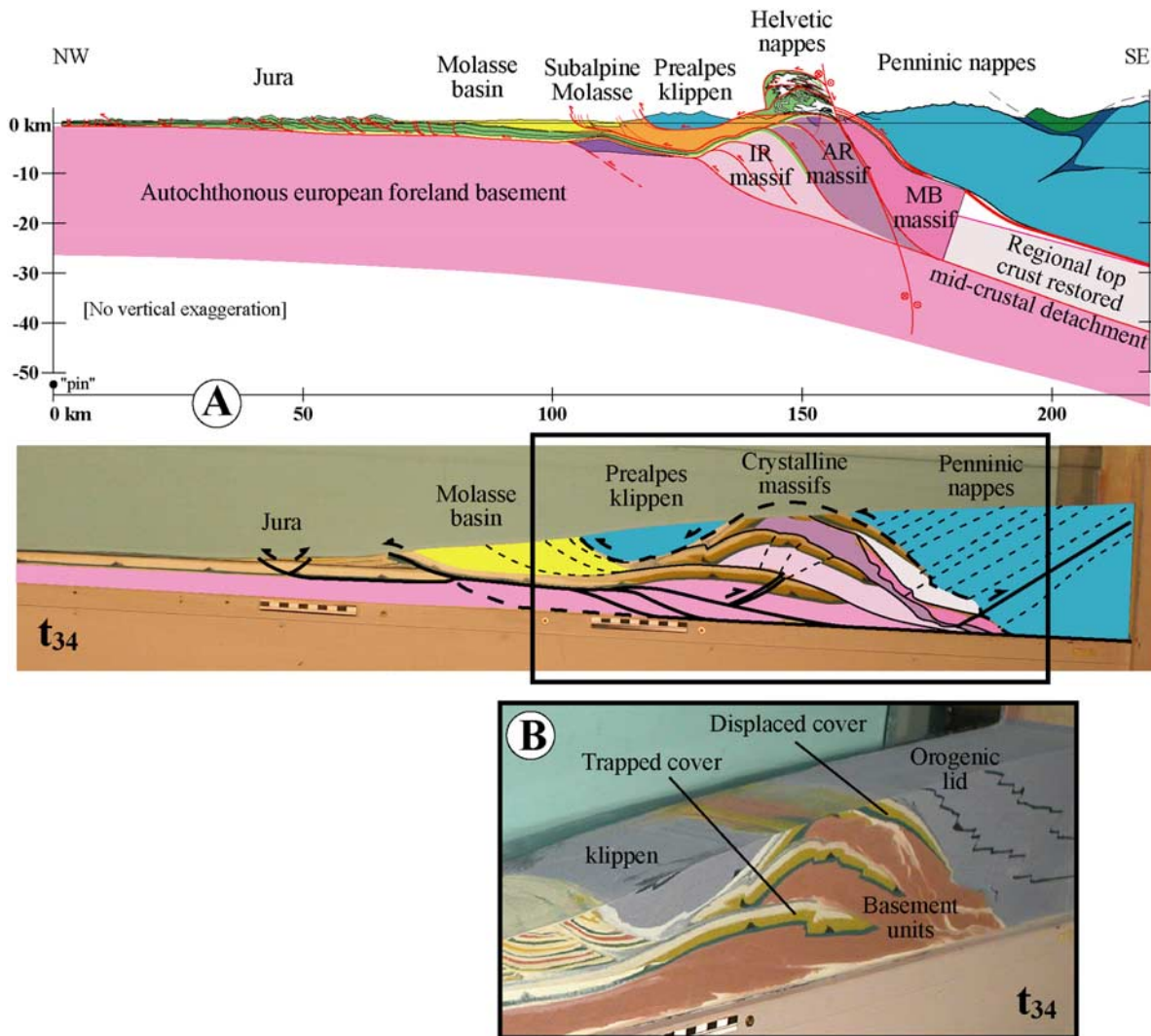


Figure 5. Comparison between the cross section by *Burkhard and Sommaruga* [1998] and the analogue model at an advanced stage of its evolution (t_{34}). (a) The two profiles are similarly color coded and the varying units are from left (NW) to right (SE): the fold-and-thrust belt of the Jura (just initiated in the experiment), the slightly deformed Molasse Basin (yellow), the Prealpes klippen (blue) separated from the lid owing to the uplift of the Crystalline Massifs (white and variations of pink) that constitute an antiformal nappe stack and the Penninic nappes (blue), remains of the lid deformed by diffuse backthrusting. (b) Common features between the antiformal nappe stack in the scheme by *Burkhard and Sommaruga* [1998] and the analogue experiment: some trapped cover between the basement imbricates, a considerable shortening accommodated on the different thrust planes, and an extensive displacement of the cover of the two most internal basement units (corresponding to the Helvetic nappes).

experimental klippen not only thrust the foreland sediments, but also lies directly on some slices of cover trapped between the basement imbricates. This observation raises the still currently debated question of the geometry and the thickness of Molasse sediments below the Prealpes klippen.

[35] Despite a difference in extent of the foreland sediment basin, the geometry of the latter is quite comparable in the model and in nature (Figure 5a). The sediments are slightly deformed owing to the brief activation of successive small thrusts propagating from the base of the basin, in response to the thrusting of the lid.

[36] The most external unit and youngest unit that appeared in the model during a new stage of frontal accretion, is considered to be the foreland fold-and-thrust belt (Figure 5a). After a long steady state period, the wedge grows by underplating and subsequent uplift of basement units. To diminish the surface slope of the taper, the wedge propagates into the foreland. The fold-and-thrust development is the combined result of the presence of a glass bead layer below the basement cover and the thickness of sediment deposits in the basin. The weak layer modifies the mechanics and the dynamics of the wedge and the

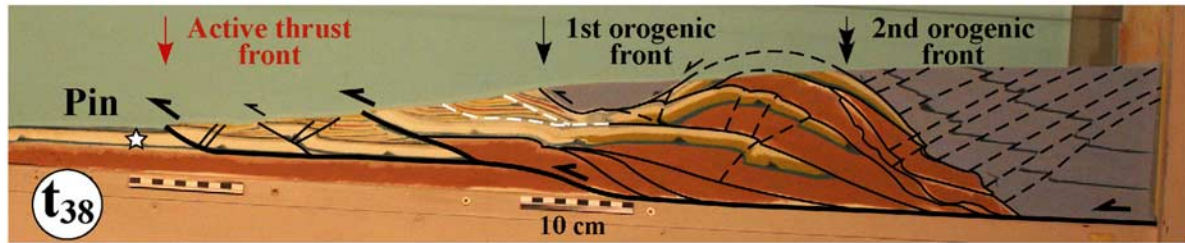


Figure 6. Location of the three studied thrust fronts separating the main tectonic units on the experimental final stage picture (t_{38}). The active thrust front (red arrow) is the last initiated thrust in the foreland, the first orogenic front represents the most advanced point of the lid (single black arrow), and the second orogenic front (double black arrow) corresponds to the front of the remaining lid, after the detachment of the frontal nappe (at t_{29}). Displacements are measured from a mobile pin (white star) located in the undeformed part of the converging plate cover.

weight of sediments favors its activation as décollement. These mechanical changes induce the forward migration of the deformation front, from a position close to the tip of the orogenic lid to a more distal position. More importantly, it is linked to the development of a basement imbricate in the not prestructured basement and the detachment occurs at the base of the autochthonous sediments unlike up to now at the base of the foreland basin sediments. This event can be compared to the “jump” of the Alpine thrust front by about 100 km northwestward, approximately from Lausanne to the external Jura, that occurred after the Serravalian (~ 12 Ma) [Burkhard and Sommaruga, 1998] and that initiated the formation of the Jura fold-and-thrust belt. The shorter distance in the model compared to the Alpine setting may be related to the influence of the evaporitic décollement level and the rheology chosen for the sedimentary series in the autochthonous. We observed subsequently in the experiment that the foreland basin migrated farther to the external domain. The remnant sedimentary basin is passively incorporated in the wedge and is largely eroded from this time on.

4.2. Interactions Between Mechanics and Surface Processes

[37] The experimental data are analyzed in a quantitative manner and presented in graphs scaled to nature.

4.2.1. Propagation of the Thrust Fronts

[38] During the experiment, we studied the progression of three specific thrust fronts separating the main tectonic units. The active thrust front which corresponds to the last initiated thrust in the foreland is illustrated by the red arrow on the final stage picture (t_{38}) (Figure 6). The first orogenic front represents the most external point of the orogenic lid in direction of the foreland and is shown by the single black arrow (Figures 6 and 7). From the stage t_{29} , it corresponds to the thrust front of the isolated nappe detached from the lid. A second orogenic front appears after the division of the lid into two distinct nappes occurs, and is illustrated by the double black arrow (Figures 6 and 7). It corresponds to the front of the remaining lid. We measured the distance of the three fronts from a pin located in the undeformed part of the converging plate cover (Figure 6), at each increment of displacement of the subducting plate (Figure 7). To favor a

direct comparison of the experimental thrust propagation to the Alpine setting, we named “active Alpine thrust”, the active thrust front, and respectively, “Penninic front” and “2nd Penninic front,” the two orogenic fronts (Figures 6 and 7).

[39] The propagations of both “Penninic” fronts are very regular (Figure 7) owing to the passive transport of the lid on the subducting plate. The active “Alpine” front (Figure 7) shows a punctuated behavior with the development of successively active frontal thrust slices at the leading edge of the wedge (green arrows in Figure 7). The cyclic development of thrust slices is expressed by a two-speed displacement of the active front illustrated by the two different slopes of the curve (Figure 7).

[40] Frontal accretion is responsible for thrust activation in the foreland basin. Thus, for example, at the stage t_{23} (Figure 7), a new thrust slice affecting the foreland sediments develops. The punctuated development of thrusts in the foreland combined with syndeformational erosion of the sediments lead to a major cyclic foreland sediment disappearance. This observation supports the conclusion proposed by Burkhard and Sommaruga [1998] that the present-day Molasse Basin is only a small remnant of a much larger foreland basin in a very advanced stage of its evolution. The basin would have been cannibalized since the early Tortonian. In the field, this volume of eroded Molasse sediments would disappear from the geological record without leaving a trace. This is suggested by burial data provided by vitrinite reflectance [Schegg et al., 1997]. As assumed by Burkhard and Sommaruga [1998], we believe that the original lengths and the total Alpine shortening on restored cross sections are underestimated. The Molasse foreland basin is most likely the structure on which the underestimation of shortening is the strongest. The erosion of a large thickness of sediments has definitively removed the structures accommodating the displacement.

[41] At the stage t_{29} (Figure 7), a new frontal thrust slice appears in the foreland but it now also affects the autochthonous cover. With no preexisting fault simulated by glass beads, the thrust is generated by the spontaneous basement underplating of the subducting plate, called “Autochthonous European basement” in reference to the cross section

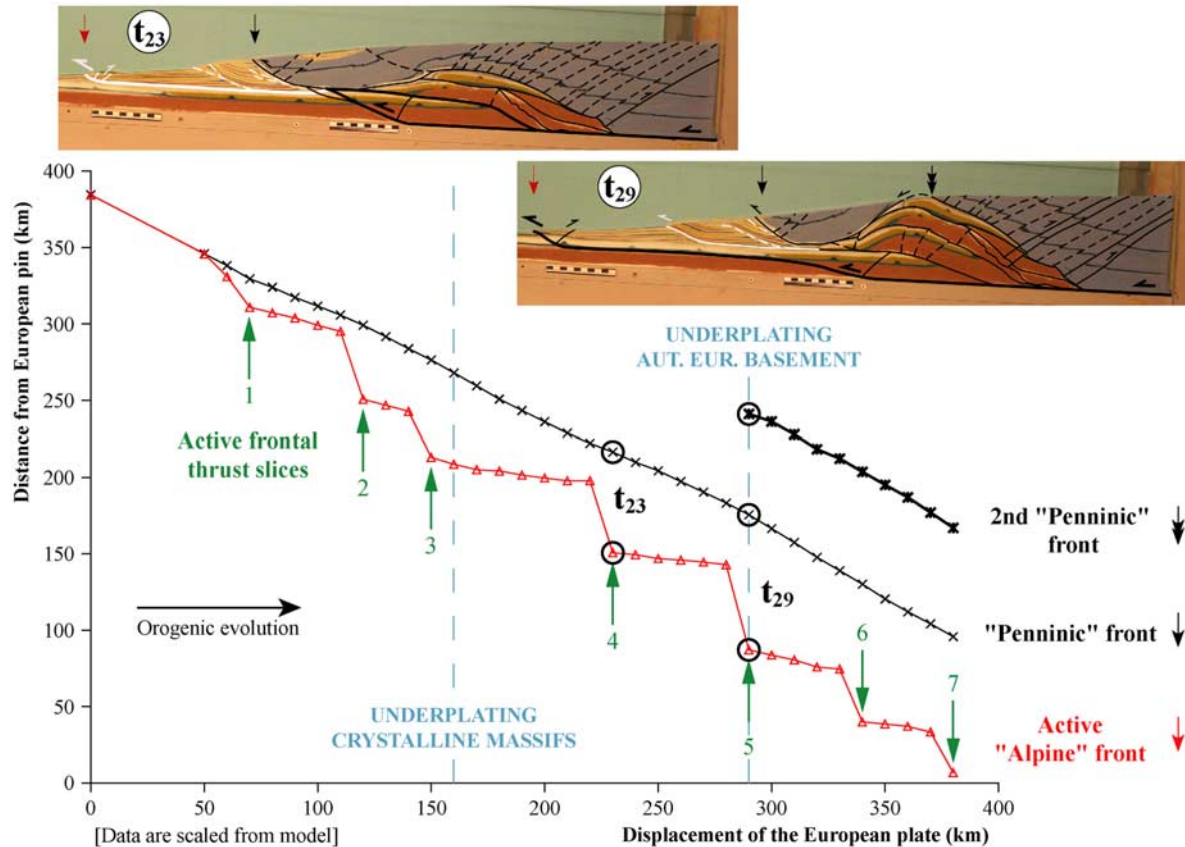


Figure 7. Propagation of the three studied fronts measured from the European pin at each step of displacement of the subducting plate. Black circles on each curve indicate the stages of development t_{23} and t_{29} illustrated by the photographs of the model. The first and the second orogenic (or “Penninic”) fronts (black curves) move very regularly owing to the passive transport of the lid on the converging plate. The propagation of the active (“Alpine”) thrust front (red curve) is in contrast punctuated by the apparition of successively active frontal thrust slices (green arrows). At t_{23} , the active front “jumps” to the foreland, leading to the development of a new thrust slice of deposited sediments. At t_{29} , the active front “jumps” again to the foreland, but the thrust is generated by the spontaneous failure of the basement also affecting the cover.

by Burkhard and Sommaruga [1998]. The mechanics of the wedge is then modified because the deformation is propagated to the foreland.

[42] We observe in the model that frontal accretion and underplating are active simultaneously. Frontal accretion in the external parts will lead to the development of a foreland fold-and-thrust belt, while underplating in the internal zones leads to the formation of the antiformal basement nappe stack. The development of the nappe stack is initiated by the tectonic inheritance of the basement, but is maintained and reinforced by the surface processes. Erosion of the lid favors and localizes the exhumation of basement imbricates and sedimentation in the foreland inhibits the lateral growth of the stack.

4.2.2. Evolution of Foreland Basin Width

[43] During the experiment, we measured the length (width) of the sedimentary foreland basin (Figure 8) including the parts thrust by the orogenic lid, thus providing the

maximal geographical extent of the basin at each stage of its evolution.

[44] The history of the basin can be divided into two stages. First, the basin is massively and constantly filled to recover the equilibrium profile of the wedge. Indeed, as the lid thrust the subducting plate, its frontal part advances and is uplifted. To maintain the initial slope of the wedge, the front of the lid is eroded and layers of sand are successively deposited in the foreland. The wedge spreads and the basin reaches its maximal length of about 130 km (Figure 8), after a displacement of 160 km of the European plate. The second stage starts with the underplating of the basement and shows a continuous slight decrease in length of the basin (Figure 8). The exhumation of the basement units modifies the development of the wedge: it does not grow anymore in length but in thickness. The layers of sand simulating the foreland sediments in the basin become shorter and thicker. At the end of the basin evolution (Figure 8), its length is approximately 110 km.

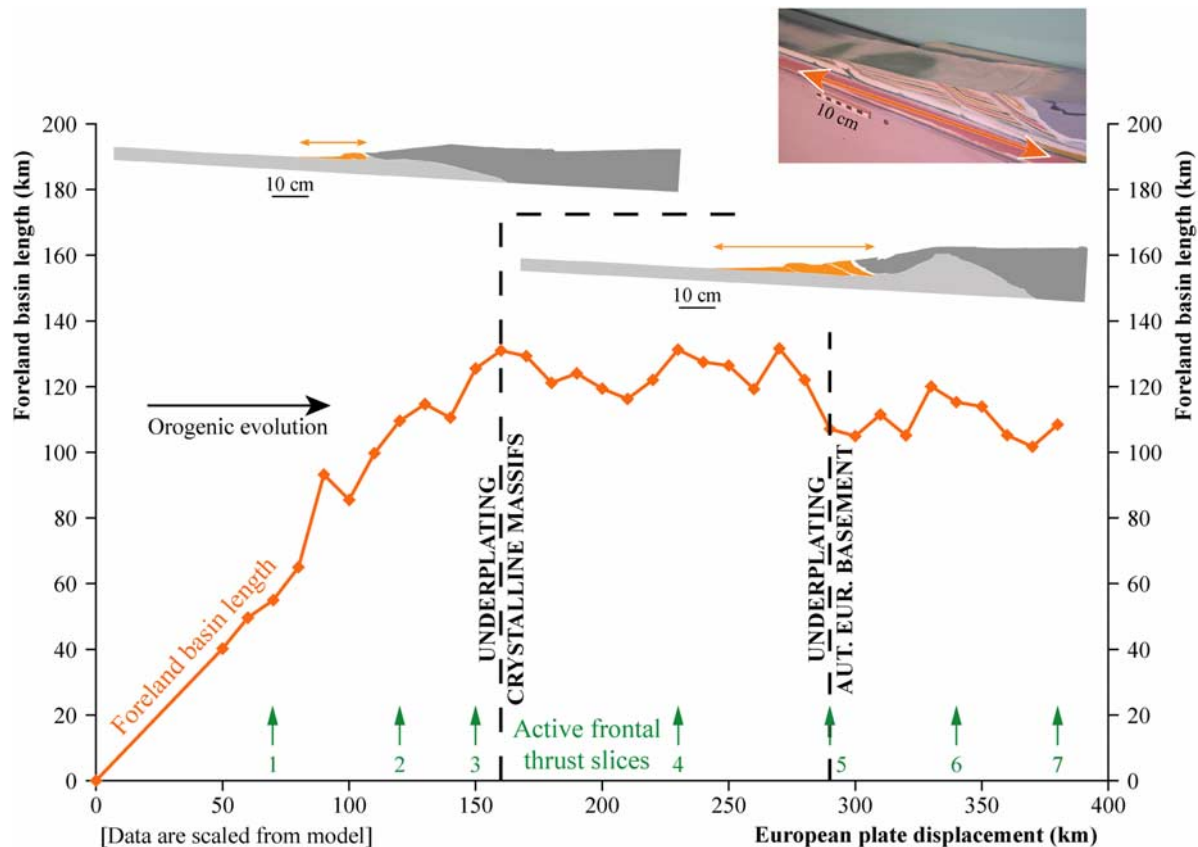


Figure 8. Length of the sedimentary foreland basin (orange curve) measured at its base (picture) at each step of displacement of the subducting plate. Two stages, each one illustrated by a scheme, are distinguishable: First, the basin is massively filled and reaches its maximal length of 130 km at 160 km of converging plate displacement and then, simultaneously with the underplating of the basement imbricates, the length of the basin slightly decreases to 110 km.

4.2.3. Sediment Budget: A Semiquantitative Study of the Experimental Results

[45] Our semiquantitative estimates of the sediment budget on the cross section (Figure 9) are expressed, scaled to the nature, in square kilometers. The data are given at each step of displacement of the subducting plate. The sedimentation rate corresponds to the surface of the last sand layer deposited in the foreland basin. The erosion rate includes all the eroded materials: first it involves mainly materials from the lid, then are added basin sediments and finally small percentages of basement units and their cover. Both curves are not cumulative, rather they express the temporal evolution of the erosion and sedimentation rates.

[46] The sedimentation rate (Figure 9) shows the same evolution as the basin length previously described: after a rapid increase it diminishes gently. In contrast, the erosion rate (Figure 9) increases rapidly, and after the initiation of underplating, strongly fluctuates around a high average value. The trend of the curves of erosion and sedimentation are then inverted and the erosive phenomenon dominates. Indeed, the rapid uplift of the prestructured basement units brings on an overelevation of the lid. To recover a stable

taper, the erosion undergoes a major increase in rate. In contrast, after the initiation of underplating, the orogenic wedge does not grow anymore and the volume of sediment deposits diminishes gradually. In nature, the barrier created by this uplift would probably restrain the sedimentary flux in the foreland, leading to an additional decrease of the sedimentation rate. Therefore it appears that the rates and the localization of sedimentation and erosion obey to the direct influence of the tectonic development to maintain the dynamics of the wedge. The cyclic secondary variations in rates of erosion, but also in sedimentation can possibly be linked to the punctuated activation of new frontal thrusts in the foreland (black arrows in Figure 9) and reflect a response to the mechanical adjustments inside the wedge.

[47] At the end of the experiment, we have estimated the whole eroded surface of the lid and the sedimented materials present on the geological record. The sediments constitute approximately 15% of the eroded materials in the lid and 43% of the original Penninic lid still remain. These estimations seem to be in a good agreement with the values proposed for the Alps [Kuhlemann *et al.*, 2002]. A more detailed discussion of model results compared with the

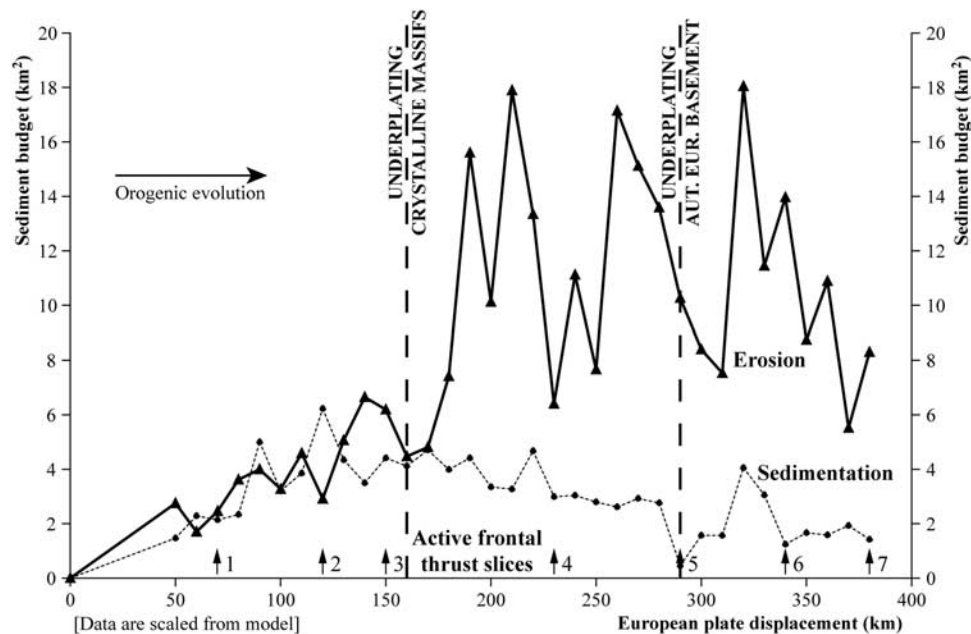


Figure 9. Sediment budget (i.e., variations in rates of erosion and sedimentation) measured in the experiment at each step of displacement of the subducting plate. The sedimentation rate (thin dashed curve) increases and after reaching its maximum, diminishes gently. In contrast, the erosion rate (thick continuous curve) increases and then strongly fluctuates around a high average value. The underplating of basement units seems to govern the rates of surface processes: The initiation of underplating modifies the trend of the curves of erosion and sedimentation and inverts their respective importance with a domination of the erosive phenomenon until the end of the experiment. The punctuated thrusting in the foreland is indicated by black arrows labeled 1 to 7.

Alpine sediment budget will be presented in a complementary work.

5. Conclusions

[48] In order to investigate the Molasse Basin evolution and the development of the outer part of the Alpine orogen along a section in Western Switzerland, we used analogue modeling to test a series of parameters and mechanisms. Our models are based on few simple, first-order assumptions: four different kinds of lithologies are simulated and we have taken into account only the upper part of the crust but not the lithosphere flexure. Most importantly, the structural inheritance of the basement and cover units was taken into account by introducing discontinuities representing inherited normal faults. The geodynamic context we intended to model corresponds to the formation of an underfilled foreland Flysch-type basin and its transition to an overfilled Molasse-type basin. Following a series of test experiments we chose one model, described herein, to discuss the importance of erosion and sedimentation on the evolution of the developing orogenic wedge. Erosion is applied to maintain a constant wedge slope and sedimentation is done in the foreland in response to changes in the wedge size. Despite the simplifications, the development of the model shows enough similarities with the complex natural cross section to draw conclusions on the evolution of the Alpine orogen and the importance of surface processes on the tectonic evolution.

[49] Modeling reveals that two major types of mechanisms are active simultaneously: frontal accretion in the external parts leading to the development of a foreland thrust belt and underplating in the internal zones leading to the formation of an antiformal nappe stack. The basement imbricates in the antiformal stack are progressively steepened during its development. In the internal part of the Alpine belt, the originally shallow SE dipping axial surfaces and thrusts in the nappe stack also steepens to become subvertical to overturned dips. The reason for this geometry, as for example proposed by *Escher et al.* [1997], is the addition by accretion through tectonic underplating of frontal imbricates resulting in the rotation of the older trailing thrust sheets.

[50] The sequential development in our model can also be favorably compared with the evolution of the stacking of the external basement massifs, the Molasse Basin development and the initiation of the Jura fold-and-thrust belt. Stacking of prestructured basement units leads to important uplift creating topography which in turn causes higher erosion to maintain the overall wedge geometry. The developing geometries are linked to the preexisting structures. The propagation of the deformation to the unstructured basements causes a shift in the foreland tectonics, where a basal décollement beneath the autochthonous sediments causes the orogenic front to “jump” away from the orogen. This is similar to the initiation of the Jura, which can therefore be correlated with the development of basement nappes.

[51] In our model, the foreland basin is partially caused by the tilt of the model setup thus creating accommodation space for sediments in front of the growing wedge. The foreland basin evolves as part of the overall orogenic wedge. Flexural bending, which was not modeled here, is another major mechanism creating accommodation space; it also possibly could help reduce the surface slope of our modeled foreland basin to shallower values, less than 2° – 4° , while keeping the overall wedge angle the same. The width of the developing basin grows to a threshold width which is achieved by the moment underplating starts, and remains more or less constant thereafter. Simultaneously, erosion reaches a maximum value. In the experiment, as in the Alpine case, important volumes of material are eroded out of the geological record and/or leave the system. The newly deposited sediments are deformed by the development of punctuated frontal thrust (due to frontal accretion) mainly during the time when underplating of prestructured basement units occurs. Some of the newly developed tectonic units are subsequently eroded, leaving uncertainties as to their original length. This observation reinforces the conclusion proposed by Burkhard and Sommaruga [1998] that the present-day Molasse Basin is only a remnant of a much larger foreland basin. As a consequence, the original lengths and the total Alpine shortening on restored cross sections are most likely underestimated. The models show that in a given setup, feedback mechanisms linking surface processes to tectonic processes are responsible for the shaping and evolution of the foreland basin. Tectonic events in the basin can be correlated with tectonics in the hinterland. The main tectonic events also lead to the major changes in the foreland basin.

[52] It appears in the experiment that to maintain the dynamics of the wedge, the surface processes obey to the direct influence of tectonic events. For instance, the initiation of basement underplating totally inverts the respective

importance of erosion and sedimentation. The overelevation of the lid due to the rapid uplift of basement imbricates is controlled by a major increase of the erosion rate. In contrast, as the orogenic wedge does not grow anymore, the volume of sediment deposits diminishes gradually. In nature, the barrier created by this uplift would probably restrain the sedimentary flux in the foreland leading to an additional decrease of the sedimentation rate. In contrast, we saw that erosion and sedimentation influence in return the tectonic development. For instance, the erosion of the lid favors a localized exhumation on prestructured basement imbricates and controls the uplift rate. The sedimentation in the foreland changes also the dynamics of the wedge. Sediment deposits inhibit the lateral development of the stack but favor the activation as décollement of the weak layer at the base of the cover, leading to the growth of the fold-and-thrust belt. The tectonic development constrains the sediment budget in space, time and rate, and vice versa.

[53] Our experimental approach shows the necessity to combine studies of erosion, sedimentation and tectonics, based on model setups including inherited structures in order to understand the feedback mechanisms involved in orogenic mountain belts such as the Alps. Studies on material paths and exhumation can be correlated with the tectonic stages, and comparisons of our experimental sediment budget with sediment/erosion budgets in Alpine-type settings have been done, but are beyond the scope of this paper and are discussed elsewhere.

[54] **Acknowledgments.** This work was supported by the University of Fribourg (Switzerland) and by a dual Ph.D. grant from the Ministère délégué à l'Enseignement supérieur et à la Recherche (France). We are grateful to A. Sommaruga and S. Willett for their comments and constructive suggestion that helped improve the manuscript. The authors would like to acknowledge Martin Burkhard, who died an untimely death while sampling in the Alps in August 2006, for the many interesting and stimulating discussions.

References

- Beaumont, C., et al. (1996), Mechanical model for subduction-collision tectonics of Alpine-type compressional orogens, *Geology*, **24**, 675–678.
- Beaumont, C., et al. (2000), Coupled tectonic-surface process models with applications to rifted margins and collisional orogens, in *Geomorphology and Global Tectonics*, edited by M. A. Summerfield, pp. 29–55, John Wiley, Hoboken, N. J.
- Boyer, S. E., and D. Elliott (1982), The geometry of thrust systems, *AAPG Bull.*, **66**, 1196–1230.
- Burkhard, M. (1988), L'Helvétique de la bordure occidentale du massif de l'Aar (évolution tectonique et métamorphique), *Eclogae Geol. Helv.*, **81**, 63–114.
- Burkhard, M. (1990), Aspects of large-scale Miocene deformation in the most external part of the Swiss Alps (Subalpine Molasse to Jura fold belt), *Eclogae Geol. Helv.*, **83**, 559–584.
- Burkhard, M., and A. Sommaruga (1998), Evolution of the Swiss Molasse basin: Structural relations with the Alps and the Jura belt, *Geol. Soc. Spec. Publ.*, **134**, 279–298.
- Buxtorf, A. (1916), Prognosen und Befunde beim Hauensteinbasis- und Grencherberg-tunnel und die Bedeutung der Letzeren für die Geologie des Juragebirges, *Verh. Naturforsch. Ges. Basel*, **27**, 184–185.
- Byrne, D. E., D. M. Davis, and L. R. Sykes (1988), Loci and maximum size of thrust earthquakes and the mechanics of the shallow region of subduction zones, *Tectonics*, **7**, 833–857.
- Cederbom, C. E., et al. (2004), Climate-induced rebound and exhumation of the European Alps, *Geology*, **32**, 709–712.
- Cobbold, P. R., et al. (2001), Sandbox modelling of thrust wedges with fluid-assisted detachments, *Tectonophysics*, **334**, 245–258.
- Dahlen, F. A. (1984), Noncohesive critical Coulomb wedges: An exact solution, *J. Geophys. Res.*, **89**, 10,125–10,133.
- Dahlen, F. A., J. Suppe, and D. Davis (1984), Mechanics of fold and thrust belts and accretionary wedges: Cohesive Coulomb theory, *J. Geophys. Res.*, **89**, 10,087–10,101.
- Dal Piaz, G. V., et al. (1972), La zona Sesia-Lanzo e l'evoluzione tettonico-metamorfica delle Alpi nordoccidentali interne, *Mem. Soc. Geol. Padova*, **32**, 1–16.
- Davis, D. M., J. Suppe, and F. A. Dahlen (1983), Mechanics of fold and thrust belts and accretionary wedges, *J. Geophys. Res.*, **88**, 1153–1172.
- Escher, A., and C. Beaumont (1997), Formation, burial and exhumation of basement nappes at crustal scale: A geometric model based on the Western Swiss-Italian Alps, *J. Struct. Geol.*, **19**, 955–974.
- Escher, A., et al. (1993), Nappe geometry in the western Swiss Alps, *J. Struct. Geol.*, **15**, 501–509.
- Escher, A., et al. (1997), Geologic framework and structural evolution of the western Swiss-Italian Alps, in *Deep Structure of the Swiss Alps—Results from NRP 20*, edited by O. A. Pfiffner et al., pp. 205–222, Birkhäuser AG, Basel, Switzerland.
- Funk, H., and B. Loup (1992), Mesozoic subsidence analysis from the Jura to the Helvetic realm, *Eclogae Geol. Helv.*, **85**, 774–775.
- Gorin, G. E., et al. (1993), Structural configuration of the western Swiss Molasse Basin as defined by reflection seismic data, *Eclogae Geol. Helv.*, **86**, 693–716.
- Guellec, S., et al. (1990), Neogene evolution of the western Alpine foreland in the light of ECORS data and balanced cross sections, in *Deep Structure of the Alps, Mem. Soc. Geol. Suisse*, vol. 1, edited by F. Roure et al., pp. 165–184, Swiss Geol. Soc., Zurich, Switzerland.
- Gutscher, M.-A., et al. (1996), Cyclical behavior of thrust wedges: Insights from high basal friction sandbox experiments, *Geology*, **24**, 135–138.
- Gutscher, M.-A., N. Kukowski, J. Malavieille, and S. Lallemand (1998a), Episodic imbricate thrusting and underthrusting: Analog experiments and mechanical analysis applied to the Alaskan

- Accretionary Wedge, *J. Geophys. Res.*, **103**, 10,161–10,176.
- Gutscher, M.-A., et al. (1998b), Material transfer in accretionary wedges from analysis of a systematic series of analog experiments, *J. Struct. Geol.*, **20**, 407–416.
- Herb, R. (1988), Eocaecene Paläogeographie und Paläotektonik des Helvetikums, *Eclogae Geol. Helv.*, **81**, 611–657.
- Homewood, P., and O. Lateltin (1988), Classic Swiss clastics: Flysch and Molasse—The Alpine connection, *Acta Geodyn.*, **2**, 1–11.
- Homewood, P., et al. (1989), Le bassin molassique Suisse, in *Dynamique et méthodes d'étude des bassins sédimentaires*, edited by Assoc. Sédim. Française, pp. 299–314, Technip, Paris.
- Hooke, R. L. (2003), Time constant for equilibration of erosion with tectonic uplift, *Geology*, **31**, 621–624.
- Hoth, S., et al. (2004), Influence of erosion on the kinematics of divergent orogens: Results from scaled sandbox-simulations, *Spec. Pap. Geol. Soc. Am.*, **398**, 201–225.
- Hunziker, J. C., et al. (1989), Alpine thermal evolution in the central and western Alps, *Geol. Soc. Spec. Publ.*, **45**, 353–367.
- Hunziker, J. C., et al. (1992), Thirty-two years of geochronological work in the central and western Alps: A review on seven maps, *Mem. Geol. Lausanne*, **13**, 1–52.
- Konstantinovskaia, E., and J. Malavieille (2005), Erosion and exhumation in accretionary orogens: Experimental and geological approaches, *Geochem. Geophys. Geosyst.*, **6**, Q02006, doi:10.1029/2004GC000794.
- Kooi, H., and C. Beaumont (1996), Large-scale geomorphology: Classical concepts reconciled and integrated with contemporary ideas via a surface process model, *J. Geophys. Res.*, **101**, 3361–3386.
- Kuhlemann, J. (2000), Post-collisional sediment budget of circum-Alpine basins (central Europe), *Mem. Soc. Geol. Padova*, **52**, 1–91.
- Kuhlemann, J., and O. Kempf (2002), Post-Eocene evolution of the north Alpine Foreland Basin and its response to Alpine tectonics, *Sediment. Geol.*, **152**, 45–78.
- Kuhlemann, J., et al. (2001), Quantifying tectonic versus erosive denudation by the sediment budget: The Miocene core complexes of the Alps, *Tectonophysics*, **330**, 1–23.
- Kuhlemann, J., et al. (2002), Post-collisional sediment budget history of the Alps: Tectonic versus climatic control, *Int. J. Earth Sci.*, **91**, 818–837.
- Kühni, A., and O. A. Pfiffner (2001), Drainage patterns and tectonic forcing: A model study for the Swiss Alps, *Basin Res.*, **13**, 169–197.
- Kukowski, N., et al. (2002), Mechanical decoupling and basal duplex formation observed in sandbox experiments with application to the Mediterranean Ridge accretionary complex, *Mar. Geol.*, **186**, 29–42.
- Lacombe, O., and F. Mouthereau (2002), Basement-involved shortening and deep detachment tectonics in forelands of orogens: Insights from recent collision belts (Taiwan, Western Alps, Pyrenees), *Tectonics*, **21**(4), 1030, doi:10.1029/2001TC901018.
- Lallemand, S. E., P. Schnürle, and J. Malavieille (1994), Coulomb theory applied to accretionary and nonaccretionary wedges: Possible causes for tectonic erosion and/or frontal accretion, *J. Geophys. Res.*, **99**, 12,033–12,055.
- Laubscher, H. P. (1973), Jura Mountains, in *Gravity and Tectonics*, edited by K. A. De Jong and R. Scholten, pp. 217–227, John Wiley, Hoboken, N. J.
- Laubscher, H. P. (1987), Die tektonische Entwicklung der Nordschweiz, *Eclogae Geol. Helv.*, **80**, 287–303.
- Laubscher, H. P. (1992), Jura kinematics and the Molasse basin, *Eclogae Geol. Helv.*, **85**, 653–676.
- Liu, H., et al. (1992), Physical models of thrust wedges, in *Thrust Tectonics*, edited by K. R. McClay, pp. 71–81, CRC Press, Boca Raton, Fla.
- Lohrmann, J., et al. (2003), The impact of analogue material properties on the geometry, kinematics and dynamics of convergent sand wedges, *J. Struct. Geol.*, **25**, 1691–1711.
- Loup, B. (1992), Evolution de la partie septentrionale du domaine helvétique en Suisse occidentale au Trias et au Lias: Contrôle par subsidence thermique et variations du niveau marin, Ph.D. thesis, Dep. Geol. Paleontol., Univ. of Geneva, Geneva.
- Malavieille, J. (1984), Modélisation expérimentale des chevauchements imbriqués: Application aux chaînes de montagnes, *Bull. Soc. Geol. Fr.*, **26**, 129–138.
- Mattauer, M. (1986), Intracontinental subduction, crust-mantle décollement and crustal-stacking wedge in the Himalayas and other collision belts, *Geol. Soc. Spec. Publ.*, **19**, 37–50.
- Molnar, P., and H. Lyon-Caen (1988), Some simple physical aspects of the support, structure, and evolution of mountain belts, *Spec. Pap. Geol. Soc. Am.*, **218**, 179–207.
- Mosar, J. (1999), Present-day and future tectonic underplating in the western Swiss Alps: Reconciliation of basement/wrench-faulting and décollement folding of the Jura and Molasse Basin in the Alpine foreland, *Earth Planet. Sci. Lett.*, **173**, 143–145.
- Mosar, J., et al. (1996), Western Préalpes médianes: Timing and structure—A review, *Eclogae Geol. Helv.*, **89**, 389–425.
- Mugnier, J.-L., et al. (1990), Crustal balanced cross-sections through the external Alps deduced from the Ecos profile, in *Deep Structure of the Alps*, *Mem. Soc. Geol. Suisse*, vol. 1, edited by F. Roure et al., pp. 203–216, Swiss Geol. Soc., Zurich, Switzerland.
- Mulugeta, G. (1988), Modelling the geometry of Coulomb thrust wedges, *J. Struct. Geol.*, **10**, 847–859.
- Naef, H., et al. (1985), Sedimentation und Tektonik im Tertiär der Nordschweiz, technical report, Nagra, Baden, Germany.
- Persson, K. S., and D. Sokoutis (2002), Analogue models of orogenic wedges controlled by erosion, *Tectonophysics*, **356**, 323–336.
- Pfiffner, O. A. (1986), Evolution of the north Alpine foreland basin in the central Alps, *Spec. Publ. Int. Assoc. Sedimentol.*, **8**, 219–228.
- Pfiffner, O. A., W. Frei, P. Valasek, M. Stauble, L. Levato, L. Dubois, and S. M. Schmid (1990), Crustal shortening in the alpine orogen: Results from deep seismic reflection profiling in the eastern Swiss Alps line NFP 20-east, *Tectonics*, **9**, 1327–1355.
- Pfiffner, O. A., S. Ellis, and C. Beaumont (2000), Collision tectonics in the Swiss Alps: Insight from geodynamic modeling, *Tectonics*, **19**, 1065–1094.
- Pfiffner, O. A., F. Schlunegger, and S. J. H. Buitert (2002), The Swiss Alps and their peripheral foreland basin: Stratigraphic response to deep crustal processes, *Tectonics*, **21**(2), 1009, doi:10.1029/2000TC900039.
- Platt, J. P. (1986), Dynamics of orogenic wedges and the uplift of high-pressure metamorphic rocks, *Geol. Soc. Am. Bull.*, **97**, 1037–1053.
- Schegg, R., et al. (1997), New coalification profiles in the Molasse Basin of western Switzerland: Implications for the thermal and geodynamic evolution of the Alpine Foreland, *Eclogae Geol. Helv.*, **90**, 79–96.
- Schlunegger, F. (1999), Controls of surface erosion on the evolution of the Alps: Constraints from the stratigraphies of the adjacent foreland basins, *Int. J. Earth Sci.*, **88**, 285–304.
- Schlunegger, F., and M. Hinderer (2001), Crustal uplift in the Alps: Why the drainage pattern matters, *Terra Nova*, **13**, 425–432.
- Schlunegger, F., and M. Hinderer (2003), Pleistocene/Holocene climate change, re-establishment of fluvial drainage network and increase in relief in the Swiss Alps, *Terra Nova*, **15**, 88–95.
- Schlunegger, F., et al. (1997), Magnetostratigraphic constraints on relationships between evolution of the central Swiss Molasse basin and Alpine orogenic events, *Geol. Soc. Am. Bull.*, **109**, 225–241.
- Schlunegger, F., et al. (1998), Crustal thickening and crustal extension as controls on the evolution of the drainage network of the central Swiss Alps between 30 Ma and the present: Constraints from the stratigraphy of the North Alpine Foreland Basin and the structural evolution of the Alps, *Basin Res.*, **10**, 197–212.
- Schmid, S. M., O. A. Pfiffner, N. Froitzheim, G. Schönborn, and E. Kissling (1996), Geophysical-geological transect and tectonic evolution of the Swiss-Italian Alps, *Tectonics*, **15**, 1036–1064.
- Schmid, S. M., et al. (2004), Tectonic map and overall architecture of the Alpine orogen, *Eclogae Geol. Helv.*, **97**, 93–117.
- Sinclair, H. D. (1997), Tectonostratigraphic model for underfilled peripheral foreland basins: An Alpine perspective, *Geol. Soc. Am. Bull.*, **109**, 324–346.
- Smit, J. H. W., J. P. Brun, and D. Sokoutis (2003), Deformation of brittle-ductile thrust wedges in experiments and nature, *J. Geophys. Res.*, **108**(B10), 2480, doi:10.1029/2002JB002190.
- Sommaruga, A. (1997), *Geology of the Central Jura and the Molasse Basin: New Insight Into an Evaporite-Based Foreland Fold and Thrust Belt*, *Mém. Soc. Neuchâteloise Sci. Nat.*, vol. 12, 176 pp., Soc. Neuchâteloise des Sci. Nat., Neuchâtel, Switzerland.
- Sommaruga, A. (1999), Décollement tectoniques in the Jura foreland fold-and-thrust belt, *Mar. Pet. Geol.*, **16**, 111–134.
- Stampfli, G. M., et al. (1998a), Obduction and subduction in the western Alps, paper presented at Geological Dynamics of Alpine Type Mountain Belts Ancient and Modern, Terra Nostra, Univ. of Bern, Bern.
- Stampfli, G. M., et al. (1998b), Subduction and obduction processes in the Swiss Alps, *Tectonophysics*, **296**, 159–204.
- Steck, A., and J. Hunziker (1994), The Tertiary structural and thermal evolution of the central Alps—Compressional and extensional structures in an orogenic belt, *Tectonophysics*, **238**, 229–254.
- Storti, F., and K. R. MacClay (1995), Influence of syn-tectonic sedimentation on thrust wedges in analogue models, *Geology*, **23**, 999–1002.
- Summerfield, M. A., and N. J. Hulton (1994), Natural controls of fluvial denudation rates in major drainage basins, *J. Geophys. Res.*, **99**, 13,871–13,883.
- Trümpy, R. (1960), Paleotectonic evolution of the central and western Alps, *Geol. Soc. Am. Bull.*, **71**, 843–908.
- Trümpy, R. (1973), The timing of orogenic events in the central Alps, in *Gravity and Tectonics*, edited by K. A. De Jong and Y. Scholten, pp. 229–251, John Wiley, Hoboken, N. J.
- Trümpy, R. (1980), *Geology of Switzerland: A Guide-Book*, Wepf and Co., Basel, Switzerland.
- Wildi, W., et al. (1991), Tectonique en rampe latérale à la terminaison occidentale de la Haute Chaîne du Jura, *Eclogae Geol. Helv.*, **84**, 265–277.
- Willett, S., et al. (1993), Mechanical model for the tectonics of doubly-vergent compressional orogens, *Geology*, **21**, 371–374.
- Willett, S. D. (1992), Dynamic growth and change of a Coulomb wedge, in *Thrust Tectonics*, edited by K. R. McClay, pp. 19–31, CRC Press, Boca Raton, Fla.

C. Bonnet, Department of Earth Science, University of California, Santa Barbara, 1006 Webb Hall, Santa Barbara, CA 93106, USA. (cecile@crustal.ucsb.edu)

J. Malavieille, Geosciences Montpellier, Université Montpellier II, Place Eugène Bataillon, F-34095 Montpellier Cedex 5, France. (jacques.malavieille@gm.univ-montp2.fr)

J. Mosar, Department of Geosciences—Earth Sciences, University of Fribourg, Chemin du Musée 6, CH-1700 Fribourg, Switzerland. (jon.mosar@unifr.ch)